

A Simple Hubbard Model for the Excited States of π Conjugated -acene Molecules

Z. S. Sadeq* and J.E. Sipe

*Department of Physics, University of Toronto, 60 St. George Street, Toronto, Ontario, Canada, M5S 1A7**

(Dated: September 3, 2022)

In this paper we present a model that elucidates in a simple way the electronic excited states of π conjugated -acene molecules such as tetracene, pentacene, and hexacene. We use a tight-binding and truncated Hubbard model written in the electron-hole basis to describe the low lying excitations with reasonable quantitative accuracy. We are able to produce semi-analytic wavefunctions for the electronic states of the system, which allows us to compute the density correlation functions for various states such as the ground state, the first two singly excited states, and the lowest lying doubly excited state. We show that in this lowest lying doubly excited state, a state which has been speculated as to being involved in the singlet fission process, the electrons and holes behave in a triplet like manner.

PACS numbers: 31.15aq, 31.15vq, 31.15xm

I. INTRODUCTION

Recent interest in the photophysics of -acene compounds [1, 8, 9], specifically tetracene ($C_{18}H_{12}$), pentacene ($C_{22}H_{14}$) and hexacene ($C_{26}H_{16}$), is due in part to the possibility of using these molecules to generate two triplet excitons following the absorption of a single photon, a phenomenon known as multi-exciton generation (MEG) or singlet fission (SF). The details of this process, potentially important for improving solar cell efficiency [28], are the subject of vigorous debate. Some assert a direct mechanism is responsible [8, 9] [29], while others claim an intermediate doubly excited state is intimately involved [30]. There are some reported observations of the intermediate doubly excited state in pentacene [10] and tetracene [11], but experimental work on these systems is also controversial. Relevant to these issues, as well as to the photophysics of these compounds more generally, are the energies of the lowest lying excited states, their nature, and the transition dipole matrix elements connecting them with the ground state and with each other. Particularly important are the lowest lying singlet and triplet states, S_1 and T_1 respectively, and a low-lying state that involves two excited electron-hole pairs. In this paper we consider an approach that yields simple estimates for the wave functions of these states and the ground state, from which other properties of interest can then be deduced.

There are a number of traditional approaches used to describe these states. The Pariser-Parr-Pople (PPP) method employs an extended Hubbard model [3, 5, 7]. More complex methods of treating the many body wavefunction involve configuration interactions (CI) or strategies based on density functional theory (DFT) [1, 3, 4, 19, 22]. With all these quantum chemistry techniques one typically employs a restricted basis, considering only a small subset of the total levels of the molecule [1]. For studies focused on the low lying electronic excitations, this can be the levels close to the highest occupied molecular orbital (HOMO) and the lowest unoccupied molecular orbital (LUMO) of the molecule. The methods are com-

putationally intensive and do not produce simple expressions for the wavefunctions. Even more complicated approaches combine aspects of DFT and the Hubbard model [6].

The lack of simpler and more physically intuitive strategies to describe these states has hindered the investigation of many of the optical properties of these molecules and their lattices, the study of which would lead to a better understanding of the states themselves. The nonlinear optical properties of these molecules, for example, remain largely unexplored, and with insight into the wavefunctions of the various electronic excited states one could propose a variety of nonlinear optical experiments, involving for example the coherent control of populations and currents [2, 14–16], to probe the electronic structure further.

The approach we use in this paper borrows features from quantum chemistry strategies, but uses them in simpler ways. In these π conjugated systems, the electrons involved in the low lying excitations of the system come from p_z orbitals on the carbon backbone. These electrons can hop between each carbon atom, leading to states that are often delocalized over the entire molecule [1]. We use a tight-binding model based on these orbitals, with a simple Hubbard interaction as a correction to introduce the Coulomb repulsion; this splits the energies of the singlet and triplet states. With the use of a standard tight-binding hopping matrix element, the model involves one adjustable parameter for each molecule, the Hubbard interaction energy. Choosing a restricted basis, we set this parameter to obtain agreement with the energy difference between the S_1 state and the ground state. We find that the energy of the other low lying states, and transition dipole moment matrix elements connecting the low lying states, are often as well described in this simple approach as they are by much more numerically intensive methods. The wave functions that result are semi-analytic, and the electronic properties of the states can be easily explored. We also introduce a simple approach to characterizing the electron-electron correlations in these states, and use it to identify the nature of the states we calculate. While the approach can be used for any conjugated organic molecule, we use it in this first application to study the electronic structure of tetracene, pentacene, and hexacene.

This paper is written in five sections. In Section II we

*Electronic address: sadeqz@physics.utoronto.ca

present the model used to describe the low lying excitations of conjugated -acenes, and in Section III we outline some of the predictions for the transition energies. In Section IV we introduce and present electron correlation functions for the ground state, the first singlet and triplet states, and the first doubly excited state. In Section V we conclude.

II. MODEL

We take the Hamiltonian to be given by the sum of tight-binding and Hubbard contributions

$$H = H_{TB} + H_{Hu}, \quad (1)$$

where the tight-binding Hamiltonian is

$$H_{TB} = -t \sum_{\langle i,j \rangle, \sigma} c_{i\sigma}^\dagger c_{j\sigma}, \quad (2)$$

with σ the spin label and i, j site labels; the angular brackets indicates sum over nearest neighbors and the operators $c_{i\sigma}$ satisfy the usual anti-commutation relations, $\{c_{i\sigma}, c_{j\sigma'}^\dagger\} = \delta_{ij}\delta_{\sigma\sigma'}$. Each carbon atom is treated as a site, contributing a p_z electron. The hopping parameter t , or transfer integral, is set to $t = 2.66$ eV, the standard value for sp^2 bonded carbon [23]. The tight-binding Hamiltonian, Eq. (2), can be written in terms of the number operators associated with its eigenbasis of delocalized states,

$$H_{TB} = \sum_{m,\sigma} \hbar\omega_m C_{m\sigma}^\dagger C_{m\sigma}, \quad (3)$$

where

$$C_{m\sigma}^\dagger = \sum_i M_{im}^* c_{i\sigma}^\dagger, \quad (4)$$

$$C_{m\sigma} = \sum_i M_{im} c_{i\sigma}, \quad (5)$$

and for all m the term M_{im} is typically non-zero for all i . The new destruction and creation operators also obey the anti-commutation relations $\{C_{m\sigma}, C_{m'\sigma'}^\dagger\} = \delta_{mm'}\delta_{\sigma\sigma'}$. The ground state of H_{TB} is then

$$|0\rangle = \prod_{m=1}^{N/2} C_{m\uparrow}^\dagger \prod_{m'=1}^{N/2} C_{m'\downarrow}^\dagger |\text{vac}\rangle, \quad (6)$$

which we call the “nominal vacuum,” where $|\text{vac}\rangle$ represents the full vacuum and N is the number of electrons in the system. The set of states that are occupied in the tight-binding ground state are the filled or the “valence” orbitals and those that are not occupied in the ground state are the unfilled or “conduction” orbitals. As usual, we denote the highest occupied molecular orbital as the HOMO, and the n^{th} state below that the HOMO- n molecular orbital; similarly, we denote the lowest unoccupied molecular orbital as the LUMO, and the m^{th} state above that the LUMO+ m molecular orbital.

The use of H_{TB} alone as the molecular Hamiltonian would lead to a degeneracy between singlet and triplet states, which in fact is broken by the electron-electron repulsion. The simplest approach to take that into account is to include in Eq. (1) a Hubbard Hamiltonian,

$$H_{Hu} = U \sum_i n_\uparrow(i) n_\downarrow(i). \quad (7)$$

Here $n_\sigma(i)$ is the number operator for site i and spin σ , $n_\sigma(i) = c_{i\sigma}^\dagger c_{i\sigma}$ and $U > 0$ is the single Hubbard parameter introduced in this model.

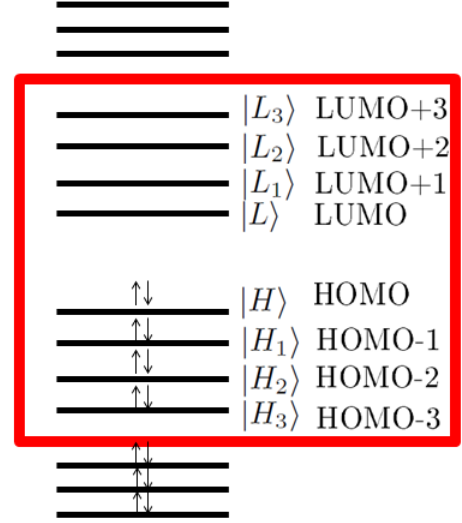


FIG. 1: Diagonalization of the tight-binding Hamiltonian leads to N electronic levels. The tight-binding ground state (see Eq. (6)) is the configuration where half the levels are filled. The red box represents the levels involved in the diagonalization of the Hamiltonian Eq. (1)

We now rewrite the total Hamiltonian (1) in the electron-hole basis. Electron creation is designated by the operator $a_{i\sigma}^\dagger$ and hole creation by $b_{i\sigma}^\dagger$, with

$$a_{L_m\sigma} \equiv C_{L_m\sigma}, \quad (8)$$

$$b_{H_n\sigma}^\dagger \equiv C_{H_n\sigma}^\dagger, \quad (9)$$

where $\tilde{\sigma}$ is the opposite spin of σ . The label L_m denotes the LUMO+ m state, and the label H_n denotes the HOMO- n state (see Fig 1); the LUMO state itself is denoted as L_0 and the HOMO state as H_0 , or for simplicity L and H respectively. The full form of the Hamiltonian in the electron-hole basis is given in Appendix A. States constructed by letting one electron and one hole creation operator act on the nominal vacuum, Eq. (6), are called “single excitations,” and those constructed by letting two electron and two hole creation operators act on the nominal vacuum, Eq. (6), are called “double excitations.”

We adopt an approach from quantum chemistry and select an “active space” defined by a set of tight-binding ex-

cited states, identified by overbars. Together with the nominal vacuum (6), these tight-binding excited states will be used to approximately diagonalize the total Hamiltonian (1); the electron and hole operators that are involved in writing these tight-binding excited states are indicated in Fig. 1.

The single excitations in our active space are of the form

$$|\overline{L_m, H_n; \sigma}\rangle = a_{L_m\sigma}^\dagger b_{H_n\bar{\sigma}}^\dagger |0\rangle, \quad (10)$$

where m and n range over $\{0, 1, 2, 3\}$. Singlet and triplet states can be constructed as superpositions of these, for example

$$|\overline{S_1}\rangle = \frac{1}{\sqrt{2}} \left(a_{L\uparrow}^\dagger b_{H\downarrow}^\dagger + a_{L\downarrow}^\dagger b_{H\uparrow}^\dagger \right) |0\rangle, \quad (11)$$

$$|\overline{S_4}\rangle = \frac{1}{\sqrt{2}} \left(a_{L_1\uparrow}^\dagger b_{H_1\downarrow}^\dagger + a_{L_1\downarrow}^\dagger b_{H_1\uparrow}^\dagger \right) |0\rangle, \quad (12)$$

for two of the singlet states, and

$$|\overline{T_1^a}\rangle = \frac{1}{\sqrt{2}} \left(a_{L\uparrow}^\dagger b_{H\downarrow}^\dagger - a_{L\downarrow}^\dagger b_{H\uparrow}^\dagger \right) |0\rangle, \quad (13)$$

$$|\overline{T_1^b}\rangle = a_{L\uparrow}^\dagger b_{H\uparrow}^\dagger |0\rangle, \quad (14)$$

$$|\overline{T_1^c}\rangle = a_{L\downarrow}^\dagger b_{H\downarrow}^\dagger |0\rangle, \quad (15)$$

$$|\overline{T_4^a}\rangle = \frac{1}{\sqrt{2}} \left(a_{L_1\uparrow}^\dagger b_{H_1\downarrow}^\dagger - a_{L_1\downarrow}^\dagger b_{H_1\uparrow}^\dagger \right) |0\rangle, \quad (16)$$

$$|\overline{T_4^b}\rangle = a_{L_1\uparrow}^\dagger b_{H_1\uparrow}^\dagger |0\rangle, \quad (17)$$

$$|\overline{T_4^c}\rangle = a_{L_1\downarrow}^\dagger b_{H_1\downarrow}^\dagger |0\rangle, \quad (18)$$

for the associated triplet states [17]; here $S^2|\overline{S_i}\rangle = 0$ for $i = 1, 4$, and $S^2|\overline{T_i^j}\rangle = 2|\overline{T_i^j}\rangle$ for $i = 1, 4$ and $j = a, b, c$. The double excitations are of the form

$$|\overline{L_m, L_{m'}; H_n, H_{n'}}\rangle = a_{L_m\uparrow}^\dagger a_{L_{m'}\downarrow}^\dagger b_{H_n\downarrow}^\dagger b_{H_{n'}\uparrow}^\dagger |0\rangle, \quad (19)$$

where here m, m', n, n' all range over $\{0, 1, 2, 3\}$. In the special case where $m = m'$ and $n = n'$ we write $|\overline{2L_m H_n}\rangle$ for $|\overline{L_m L_m; H_n, H_n}\rangle$. The lowest lying state of this type, $|\overline{2LH}\rangle$, where $m = n = 0$, is sometimes referred to as $|D\rangle$ [1]. It can be written as $(a_{L\uparrow}^\dagger b_{H\uparrow}^\dagger)(a_{L\downarrow}^\dagger b_{H\downarrow}^\dagger)|0\rangle$ and from (14, 15) can be associated with the presence of two triplets.

When we diagonalize the Hamiltonian (1) in our active space we find the Hamiltonian matrix splits into two blocks, one containing only single excitations and the second containing the nominal vacuum and the double excitations. The double excitations (19) included in the active space are those that are coupled to the nominal vacuum by the Hubbard Hamiltonian. Other double excitations that can be constructed where m, m', n, n' still range over $\{0, 1, 2, 3\}$, but where either the electrons have the same spin, or the holes have the same spin, or both, are coupled to the double excitations in our active space by the Hubbard Hamiltonian. But we find expanding the active space to include them as well leads to very small changes in our results, and so we neglect them.

Upon diagonalizing the Hamiltonian we find a new ground state that we denote by $|g\rangle$; other states are labeled, without

an overbar, by the tight-binding states that contribute to them with the largest amplitude. So, for example,

$$|g\rangle = c_g^0 |0\rangle + \sum_a c_g^a |\overline{a}\rangle, \quad (20)$$

$$|S_1\rangle \approx c_1^1 |\overline{S_1}\rangle + c_1^4 |\overline{S_4}\rangle, \quad (21)$$

$$|2LH\rangle = c_{2LH}^{2LH} |\overline{2LH}\rangle + c_{2LH}^0 |0\rangle + \sum_{a \neq 2LH} c_{2LH}^a |\overline{a}\rangle, \quad (22)$$

where the c_i^j are complex numbers, the $|\overline{a}\rangle$ indicate double excitations (19), and $|c_1^1| > |c_1^4|$, etc. The scaling of energy levels with U is shown in Fig. 2 for pentacene; the plots for tetracene and hexacene are similar. In the tight-binding limit, $U = 0$, the singlet and triplet states are degenerate; as U is increased the triplet states remain degenerate but the singlet state rises faster in energy as U increases, and the energy for the $2LH$ state is least sensitive to U .

Taking the Hubbard energy U as an adjustable parameter, a reasonable strategy would be to set U so we get agreement with the experimental value of the transition energy from the ground state to S_1 . Unfortunately, we are not aware of any gas phase data published for the absorption spectrum of these molecules; this would be the most appropriate for comparison with our model of isolated molecules. Available data is for molecules in solution, except for the triplet state in pentacene, where the energy is extracted from experiments on pentacene dopants in a tetracene single crystal, interpreted with the aid of an energy transfer model [21]. The early experimental data for the singlet states of tetracene and pentacene tabulated by Yamagata *et al.* [19] is for tetracene and pentacene with a solvent of benzene, and the results of Angliker *et al.* [27] are for the singlet states of hexacene in a solvent of silicone oil. For hexacene we only report the bright singlet states, and compare to the bright singlet states measured by Angliker *et al.* [27]. For the triplet states in tetracene, the work was carried out by Völcker *et al.* in a solution of 2-methyltetrahydrofuran [20], and in pentacene the first triplet state was investigated by Burgos *et al.* [21]. In the absence of gas phase data, we set our values of U to give the correct transition energy from the ground state to S_1 of the molecules in solution.

III. ELECTRONIC STATES OF TETRACENE, PENTACENE AND HEXACENE

In Table I we present the singlet energies, and the energy for $2LH$, found from our calculations; in Table II we give the oscillator strengths for the singlet transitions, where the oscillator strength is

$$f_{qq'} = \frac{2m_e \omega_{qq'}}{3\hbar e^2} \sum_\beta |\mu_{qq'}^\beta|^2, \quad (23)$$

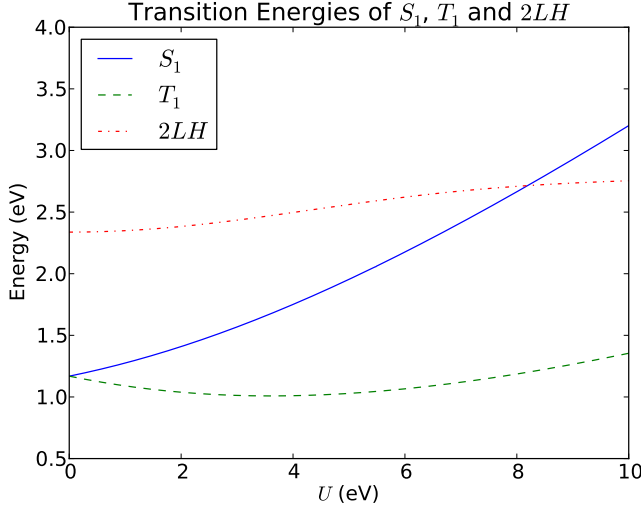


FIG. 2: Transition energies from the ground state to the first singlet, triplet, and doubly excited states in pentacene, as a function of the Coulomb repulsion parameter, U .

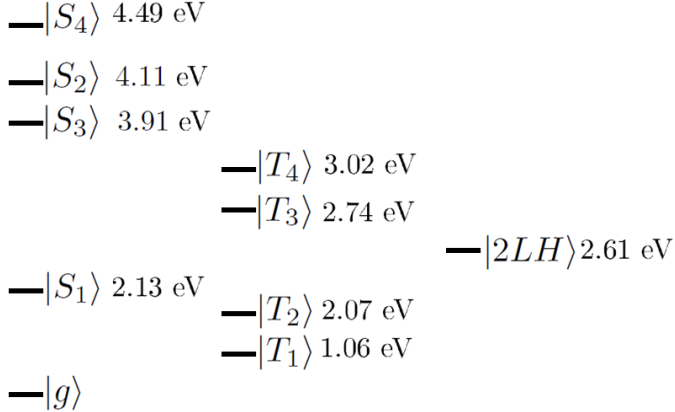


FIG. 3: Level structure of pentacene showing the first four singlet and triplet excited states as well as the first doubly excited state.

with $\omega_{qq'}$ the frequency difference between states q and q' , $\mu_{qq'}^\beta$ the β component of the transition dipole matrix element between states q and q' , and m_e the electron mass. The form of the dipole operator used to compute the transition dipole matrix elements is given in Appendix B. We assume the bond length to be uniform in all three molecules with a bond length $l = 1.42\text{\AA}$ [24]. In both tables we compare with experimental values in solution, as indicated in the figure captions, in the absence of any available gas phase data. While the energy of S_1 is in each case set to be in agreement with the experimental value by the choice of U , other energies such as S_2 , and the oscillator strengths, can be taken as predictions of our model, which of course do not include any of the solvent corrections that could be expected in the experimental data. Especially

considering this limitation, we see reasonable agreement with experimental data.

We also find reasonable agreement with quantum chemical calculations [3, 4, 19, 22], where solvent effects are also neglected, although different workers find very different energies for the same state. For example, for the energy of the S_1 state in pentacene, which is set in our model, the calculated values range from 2.31 eV to 3.33 eV [3, 4, 19, 22]. For S_2 , where subject to corrections due to solvent effects our result of 4.11 eV can be taken as a prediction, the results from more sophisticated calculations give values that range from 3.11 eV [22] to 4.23 eV [19]. The predicted values of our model typically fall within the range defined by the more sophisticated quantum chemical calculations. Similarly, there are a wide range of predicted oscillator strengths from those more sophisticated calculations; for example, Yamagata *et al.* [19] calculate a value of 0.275 for the g to S_1 transition in pentacene while Pedash *et al.* [22] calculate 0.184; we find 0.146.

The lowest energy triplets predicted by this model are presented in Table III. The level structure for pentacene is shown in Fig. 3. Note that we follow Yamagata *et al.* [19] and assign levels by comparing our calculated oscillator strengths with those determined experimentally, rather than by comparing our calculated energies with those determined experimentally; this leads to S_3 having a slightly lower energy than S_2 in tetracene and pentacene.

The singlet and triplet states are composed of states in which there is a hole in H_i and an electron in L_j ; we denote this by $H_i \rightarrow L_j$, identifying the motion of an actual electron necessary to create the single excitation from the nominal vacuum. In all molecules S_1 is made up of mostly $H \rightarrow L$. The largest contribution to S_2 is from $H_1 \rightarrow L_1$ in all molecules. However, in tetracene there is significant mixing with $H_3 \rightarrow L$ and $H \rightarrow L_3$, in pentacene there is significant mixing with $H_2 \rightarrow L$, $H \rightarrow L_2$, $H_3 \rightarrow L$ and $H \rightarrow L_3$, and in hexacene there is significant mixing with $H_2 \rightarrow L$ and $H \rightarrow L_2$. The state S_3 is composed only of

Level	Tetracene (eV)	Pentacene (eV)	Hexacene (eV)
S_1	2.61(2.61)	2.13(2.13)	1.90(1.90)
S_2	4.97(4.21)	4.11(3.58)	3.57 (3.17)
S_3	4.19(4.53)	3.91(4.07)	3.80 (3.94)
S_4	5.31(5.46)	4.49(4.34)	3.97
$2LH$	3.43	2.61	2.06

TABLE I: Energies for various levels of tetracene, pentacene and hexacene. Energies reported for these levels are the absolute energies of these states minus the absolute energy of the ground state. The Hubbard repulsion parameter was set to $U = 5.54$ eV for tetracene, $U = 5.80$ eV for pentacene and $U = 6.38$ eV for hexacene. Experimental values of the molecules in solution are indicated in brackets; those for tetracene and pentacene are from data tabulated from the literature by Yamagata *et al.* [19], where the solvent was benzene; the values for hexacene are found by Angliker *et al.* [27], where the solvent was silicone oil. We find a dark singlet state in hexacene at 2.93 eV, which Angliker *et al.* find at 2.67 eV; we do not include it in this table.

Transition	Tetracene	Pentacene	Hexacene
$g \rightarrow S_1$	0.194 (0.108)	0.146 (0.0995)	0.104 (0.100)
$g \rightarrow S_2$	0.305 (0.0998)	0.276 (0.0982)	0.252 (0.100)
$g \rightarrow S_3$	2.84 (1.75)	3.16 (2.41)	3.39 (5.00)
$g \rightarrow S_4$	0.104 (0.155)	0.0980 (0.243)	0.0575
$S_1 \rightarrow 2LH$	0.138	0.0877	0.0307

TABLE II: Table of oscillator strengths for certain transitions of tetracene, pentacene and hexacene. Experimental values of the oscillator strength of the molecules in solution are indicated by brackets; those for tetracene and pentacene are computed by Yamagata *et al.* [19] from the experimental values of the dipole matrix elements of tetracene and pentacene in a solvent of benzene; those for hexacene are measured by Angliker *et al.* [27] in a solvent of silicone oil.

Level	Tetracene (eV)	Pentacene (eV)	Hexacene (eV)
T_1	1.45 (1.35)	1.06 (0.86)	0.84
T_2	2.67	2.07	1.69
T_3	3.40	2.74	2.36
T_4	3.70	3.02	2.52

TABLE III: Energies of triplet levels in tetracene, pentacene and hexacene. Energies reported for these levels are the absolute energies of these states minus the absolute energy of the ground state. The experimental value for the first triplet state of tetracene is taken from Völcker *et al.* [20], where tetracene was studied in a solvent of 2-methyltetrahydrofuran, while that of pentacene is taken from Burgos *et al.* [21] where pentacene molecules were studied as dopants in tetracene single crystals.

$H_2 \rightarrow L$ and $H \rightarrow L_2$ in tetracene, only of $H_2, H_3 \rightarrow L$ and $H \rightarrow L_2, L_3$ in pentacene, and only of $H_3 \rightarrow L$ and $H \rightarrow L_3$ in hexacene. In all molecules, the largest contribution to S_4 is from $H_1 \rightarrow L_1$, but in tetracene there is significant mixing with $H_3 \rightarrow L$ and $H \rightarrow L_3$, in pentacene there is significant mixing with $H_2, H_3 \rightarrow L$ and $H \rightarrow L_2, L_3$, and in hexacene

there is significant mixing with $H_2 \rightarrow L$ and $H \rightarrow L_2$.

Turning to the triplets, in all molecules the state T_1 is mainly $H \rightarrow L$ and the states T_2, T_3 are made up of mostly $H_1 \rightarrow L$ and $H \rightarrow L_1$. While T_4 consists mainly of $H_1 \rightarrow L_1$ in all three molecules, there is significant mixing with $H \rightarrow L_3$ and $H_3 \rightarrow L$ in tetracene, with $H \rightarrow L_2, L_3$ and $H_2, H_3 \rightarrow L$ in pentacene, and with $H \rightarrow L_2$ and $H_2 \rightarrow L$ in hexacene.

IV. ELECTRON DENSITY CORRELATION FUNCTION

A. Ground State Electron Correlation

We now turn to the characterization of the states, and the identification of the impact of the Hubbard Hamiltonian on their nature. From a perspective of condensed matter physics, the most natural way to begin this is to consider the electron correlations. There one typically introduces a density operator $n(\mathbf{r}) = \sum_{\sigma} n_{\sigma}(\mathbf{r})$ where $n_{\sigma}(\mathbf{r})$ is the density operator associated with spin $\sigma = \uparrow, \downarrow$ and $n_{\sigma}(\mathbf{r}) = \sum_s \psi^{\dagger}(\mathbf{r}, s) \psi(\mathbf{r}, s)$ where the field operator $\psi(\mathbf{r}, s) = \sum_{\alpha, \sigma} \chi_{\sigma}(s) \phi_{\alpha}(\mathbf{r}) c_{\alpha \sigma}$, with $\chi_{\sigma}(s)$ a complete set of spinor functions, $\phi_{\alpha}(\mathbf{r})$ a complete set of wave functions, and the $c_{\alpha \sigma}$ fermion operators satisfying $\{c_{\alpha \sigma}, c_{\alpha' \sigma'}\} = 0$, $\{c_{\alpha \sigma}, c_{\alpha' \sigma'}^{\dagger}\} = \delta_{\alpha, \alpha'} \delta_{\sigma \sigma'}$. In the usual way [25, 26] we find

$$n_{\sigma}(\mathbf{r}) n_{\sigma'}(\mathbf{r}') = \delta_{\sigma \sigma'} \delta(\mathbf{r} - \mathbf{r}') n_{\sigma}(\mathbf{r}) + F_{\sigma \sigma'}(\mathbf{r}, \mathbf{r}'), \quad (24)$$

where the right-hand side follows from normal ordering the operators on the left-hand side and used the assumed completeness of the functions $\phi_{\alpha}(\mathbf{r})$ and that of the spinors $\chi_{\sigma}(s)$; here

$$F_{\sigma \sigma'}(\mathbf{r}, \mathbf{r}') = \sum_{\alpha_1, \alpha_2, \alpha_3, \alpha_4} \phi_{\alpha_1}^*(\mathbf{r}) \phi_{\alpha_3}^*(\mathbf{r}') \phi_{\alpha_2}(\mathbf{r}) \phi_{\alpha_4}(\mathbf{r}') c_{\alpha_3 \sigma'}^{\dagger} c_{\alpha_1 \sigma}^{\dagger} c_{\alpha_2 \sigma} c_{\alpha_4 \sigma'}. \quad (25)$$

The expectation value of the density-density correlation function in any pure or mixed state is then given by

$$\langle n(\mathbf{r}) n(\mathbf{r}') \rangle = \delta(\mathbf{r} - \mathbf{r}') \langle n(\mathbf{r}) \rangle + \langle n(\mathbf{r}) \rangle \langle n(\mathbf{r}') \rangle g^{(2)}(\mathbf{r}, \mathbf{r}'), \quad (26)$$

where the correlation function

$$g^{(2)}(\mathbf{r}, \mathbf{r}') = \frac{\sum_{\sigma, \sigma'} \langle F_{\sigma \sigma'}(\mathbf{r}, \mathbf{r}') \rangle}{\langle n(\mathbf{r}) \rangle \langle n(\mathbf{r}') \rangle}. \quad (27)$$

The first term on the right hand side of Eq. (26) is associated with the contribution of the “same” electron in $n(\mathbf{r})$ and $n(\mathbf{r}')$; the second term, characterized by the dimensionless quantity $g^{(2)}(\mathbf{r}, \mathbf{r}')$, describes the correlation of pairs of electrons above and beyond what one would expect simply from the varying densities. For some models, such as a noninter-

acting, or ideal, Fermi gas at zero temperature, it can be easily evaluated [26].

Here we want to associate a density operator $n_{\sigma}(i)$ for an electron with spin σ at a particular site i ,

$$n_{\sigma}(i) = c_{i \sigma}^{\dagger} c_{i \sigma} = \sum_{m m'} \Gamma_{m m'}(i) C_{m \sigma}^{\dagger} C_{m' \sigma}, \quad (28)$$

where from the inverse of Eqs. (4,5) we have

$$\Gamma_{m m'}(i) = M_{i m}^* M_{i m'}, \quad (29)$$

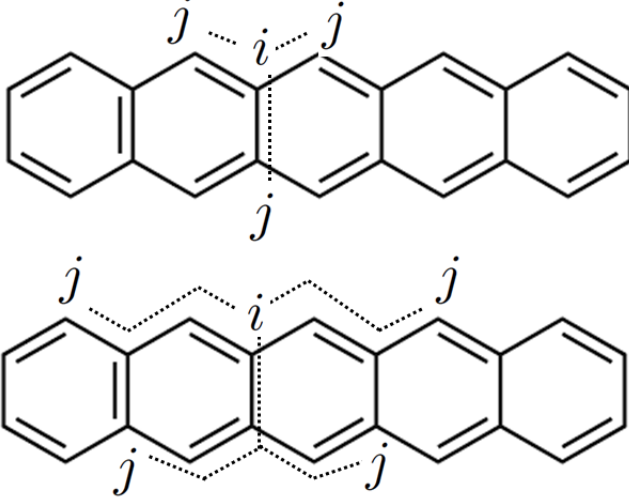


FIG. 4: A cartoon figure of pentacene and the separation of sites by different bond length distances. In the top figure, we indicate the procedure to compute $g^{(2)}(s=1)$. For the particular site i there are three sites j that contribute for $s=1$; we sum these contributions, then sum over all sites i , and finally normalize appropriately. The bottom figure shows the procedure for $s=3$. For site i the contributions from the four sites that contribute to $g^{(2)}(s=3)$ are shown in the figure.

and a total density operator at site i

$$n(i) = \sum_{\sigma} n_{\sigma}(i). \quad (30)$$

Following the strategy for the more general discussion in the previous paragraph, we find

$$n_{\sigma}(i)n_{\sigma'}(j) = \delta_{\sigma\sigma'}\delta_{ij}n_{\sigma}(i) + F_{\sigma\sigma'}(i,j), \quad (31)$$

where we have used the fact that M is a unitary matrix, and now

$$F_{\sigma\sigma'}(i,j) = \sum_{mm'pp'} \Gamma_{mm'}(i)\Gamma_{pp'}(j)C_{p\sigma}^{\dagger}C_{m\sigma}^{\dagger}C_{m'\sigma}C_{p'\sigma'} \quad (32)$$

In any pure or mixed state we then have

$$\langle n(i)n(j) \rangle = \delta_{ij}\langle n(i) \rangle + \langle n(i) \rangle \langle n(j) \rangle g^{(2)}(i,j), \quad (33)$$

where now the dimensionless quantity

$$g^{(2)}(i,j) = \frac{\sum_{\sigma\sigma'} \langle F_{\sigma\sigma'}(i,j) \rangle}{\langle n(i) \rangle \langle n(j) \rangle}, \quad (34)$$

characterizes the correlations between pairs of electrons. As in the more general discussion in the previous paragraph, in simple models this can be worked out explicitly. For example, if we neglect the Hubbard part of the Hamiltonian, Eq. (1), and consider the tight-binding ground state, we have

$$g_{TB}^{(2)}(i,j) = 1 - \frac{\sum_{lk} \Gamma_{lk}(i)\Gamma_{kl}(j)}{2 \sum_l \Gamma_{ll}(i) \sum_k \Gamma_{kk}(j)}, \quad (35)$$

where the sums over k and l extend over all filled states.

Although tabulating $g^{(2)}(i,j)$ for all pairs of sites i and j could be done, this would provide a surfeit of information. Recall that for a uniform electron gas $g^{(2)}(\mathbf{r}, \mathbf{r}')$ only depends on $|\mathbf{r} - \mathbf{r}'|$, and the correlation function can be identified by giving its dependence only on that one variable. Here things are more complicated, for $g^{(2)}(i,j)$ does not depend just on the distance between i and j , but also on where the sites i and j are located on the molecule. Further, since in our model electrons can move from one site i to another j by moving from one carbon site to another, arguably the physically relevant distance between i and j is not the actual distance between the sites but rather the minimum number of bond length steps necessary to get from i to j , s_{ij} , which we call the *bond length distance* between the sites; clearly $s_{ji} = s_{ij}$ (see Fig. 4). While $g^{(2)}(i,j)$ does not depend just on s_{ij} , we can construct an average $g^{(2)}(s)$ for the molecule by averaging over all pairs (i,j) of sites in the molecule with the same bond length distance between them. More precisely, we take

$$g^{(2)}(s) \equiv \frac{1}{\mathcal{N}(s)} \sum_{\substack{(i,j) \text{ such that} \\ s_{ij}=s}} g^{(2)}(i,j), \quad (36)$$

where $\mathcal{N}(s)$ is the number of pairs (i,j) of sites appearing in the sum. Here $s = \{0, 1, 2, \dots, s_{\max}\}$, with s_{\max} is the maximum bond length distance between pairs of sites in the molecule; s_{\max} is dependent on the molecule, and for pentacene, for example, we have $s_{\max} = 11$.

To calculate $g^{(2)}(s)$ for a particular s , we begin with a site i and find all sites j with $s_{ij} = s$; we sum $g^{(2)}(i,j)$ over those. We do this for all i and add the contributions. In doing so we have counted each pair (i,j) twice, but we then divide by the number of contributions and recover (36).

We plot $g^{(2)}(s)$ calculated from the tight-binding ground state, which we label $g_{TB}^{(2)}(s)$, where the Hubbard Hamiltonian (7) is neglected, and $g^{(2)}(s)$ calculated with the inclusion of the Hubbard Hamiltonian, which we label $g_{Hu}^{(2)}(s)$. We also define

$$\Delta g^{(2)}(s) = g_{Hu}^{(2)}(s) - g_{TB}^{(2)}(s). \quad (37)$$

This difference is also plotted in Fig. 5.

Even at the tight-binding level there is a Fermi hole as $s \rightarrow 0$, analogous to the behavior of $g^{(2)}(\mathbf{r}, \mathbf{r}')$ of Eq. (27) in an ideal Fermi gas, with $g^{(2)}(0) = 0.5$. The oscillatory behavior as a function of s in $g_{TB}^{(2)}(s)$ is analogous to the oscillation seen in $g^{(2)}(\mathbf{r}, \mathbf{r}')$ as a function of $|\mathbf{r} - \mathbf{r}'|$ for an ideal Fermi gas [25, 26]. The density correlation function for an ideal Fermi gas in one dimension is given by [26]

$$g_{1D}^{(2)}(r) = 1 - \frac{1}{4k_F^2 r^2} + \frac{\cos(2k_F r)}{4k_F^2 r^2}, \quad (38)$$

where we have defined $r \equiv |\mathbf{r} - \mathbf{r}'|$ and k_F is the Fermi wavevector. In one dimension, the wavevector k_F can be expressed as $k_F = \pi n/2$ where n is the linear density. In our model this density is one electron per unit length, $n = 1/l$,

where l is the bond distance. Therefore, we would identify an effective $k_F = \pi/2l$. One can also physically think of k_F as being related to the wavelength of oscillation of the HOMO state. The HOMO tight-binding wavefunction has a wavelength of approximately $4l$. That is, if one is constrained to move within the sites then regions of positive and negative amplitude are separated by $4l$. This also leads to the identification of an effective $k_F = \pi/2l$. So either approach leads us to expect oscillations with a period of $2l$, which is indeed observed in the plots of $g^{(2)}(s)$ in Fig. 5, where we also plot $g_{1D}^{(2)}(sl)$ and $g_{2D}^{(2)}(sl)$ as a function of s where $g_{2D}^{(2)}(sl)$ is the density correlation function for a two dimensional ideal Fermi gas. For $g_{1D}^{(2)}(sl)$ (Eq. (38)) we take the density $n = 1/l$, while for $g_{2D}^{(2)}(sl)$ we take the density to be the areal density of p_z electrons in a graphene lattice with the same l .

It is evident that including the Hubbard interaction reduces the electron density at $s = 0$, and increases it at larger s . We note that even if the size of the basis set is decreased, the behavior of $\Delta g^{(2)}(s)$ remains qualitatively the same. Such a decrease leads to an overall increase in the ground state energy, and thus $\Delta g^{(2)}(s)$ is higher at $s = 0$, but the overall pattern and oscillations remain qualitatively similar. Thus, even a smaller basis can effectively capture the physics of the ground state of the system. We expand on this in Appendix C.

Of the three -acenes, the tight-binding prediction of the HOMO-LUMO gap is closest to the singlet transition energy of hexacene, and furthest from that of tetracene. In Fig 5, we see that it is tetracene that is most affected by the Hubbard corrections, while hexacene is the least affected, as evidenced by the magnitude of the corrections in $\Delta g^{(2)}(s)$ for small s .

B. Electron-Hole Correlations in Single and Double Excited States

1. Electron Picture

We now calculate the electron density correlation (34) for three selected excited states: the first singlet state S_1 , the first triplet state T_1 , and the doubly excited state $2LH$. The $\Delta g^{(2)}(s)$ for those states, as defined again by (37), are all plotted in Figs 6, 7.

In the tight-binding model, the states S_1 and T_1 are energetically degenerate, both involving the excitation of an electron from the HOMO to the LUMO. The introduction of the Coulomb repulsion term breaks this degeneracy, with the singlet states higher in energy than the triplet states; this is seen in Fig. 2. Typically, singlet states have a spatial component of their wave function that is symmetric with respect to exchange of particle coordinates, leading to a large spatial overlap between electrons and a larger Coulomb interaction than triplet states. In our model, this manifests itself in $\Delta g^{(2)}(0)$ being greater for singlet states than triplet states. As for the ground state the magnitude of the Hubbard corrections $\Delta g^{(2)}(s)$ to $g^{(2)}(s)$ are largest for tetracene and smallest for hexacene.

The $2LH$ state (Fig 7) behaves similarly to both the ground and the first triplet state in the sense that $\Delta g^{(2)}(0)$ is negative.

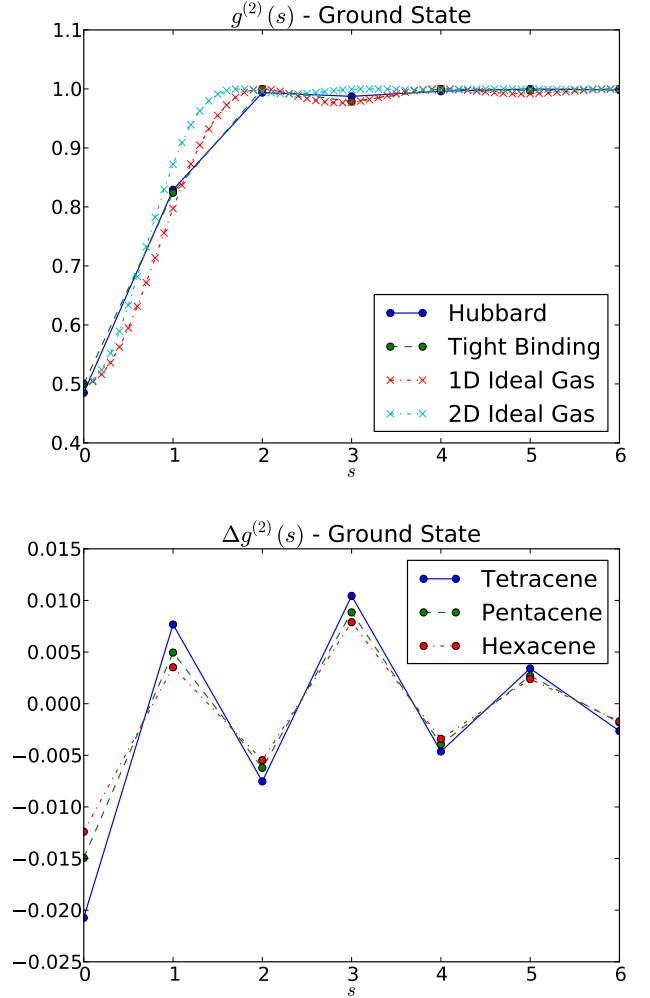


FIG. 5: (Top) The $g^{(2)}(s)$ function is plotted for the ground state in both tight-binding and Hubbard models for pentacene, along with the corresponding correlation functions for a 1D and 2D ideal gas. The Hubbard and tight-binding results are essentially indistinguishable on this scale. The quantities for tetracene and hexacene are similar. The difference between the two cases is illustrated in the quantity $\Delta g^{(2)}(s) = g_{Hu}^{(2)}(s) - g_{TB}^{(2)}(s)$ where all three molecules are shown (bottom). Both these are plotted as a function of s , which identifies the distance in multiples of the bond length.

As for the ground state, the magnitude of the Hubbard corrections $\Delta g^{(2)}(s)$ to $g^{(2)}(s)$ are largest for tetracene and smallest for hexacene.

For the $2LH$ state, reducing the size of the basis leads to qualitatively similar behavior for the $\Delta g^{(2)}(s)$; the energy difference between $2LH$ and the ground state also remains similar. Thus the essential physics of this state can be effectively captured by a smaller basis. We expand on this in Appendix C.

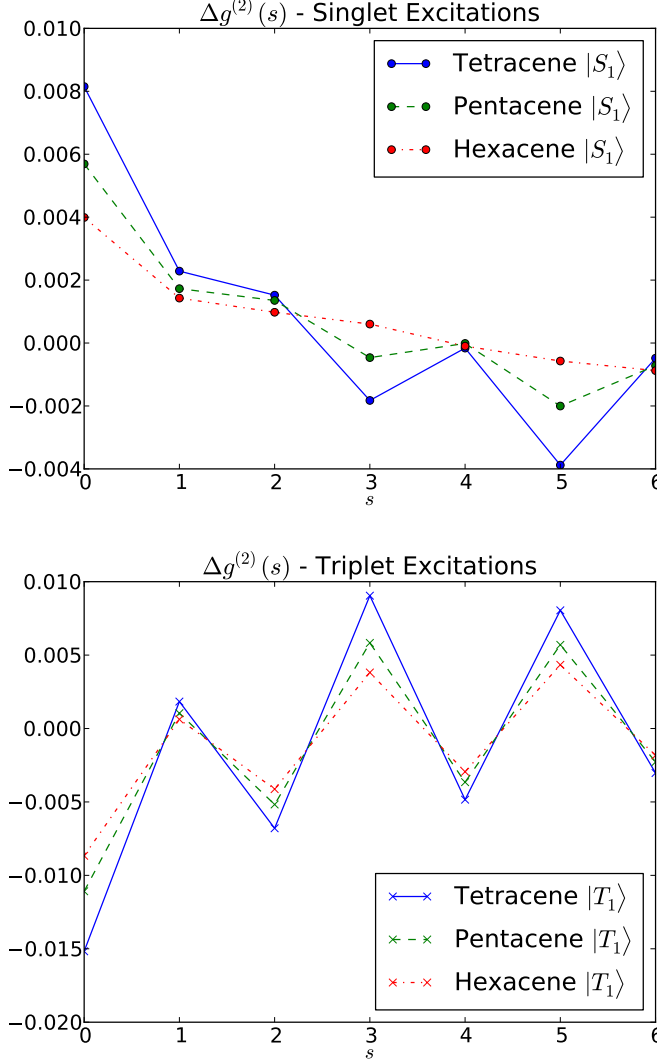


FIG. 6: $\Delta g^{(2)}(s)$ plotted for the first singlet state, $|S_1\rangle$ (top), and first triplet state, $|T_1\rangle$ (bottom) in tetracene, pentacene and hexacene. Upon the introduction of the Hubbard interaction, the electron density in the $|S_1\rangle$ state at $s = 0$ becomes larger, thereby increasing the energy. This is in contrast to the $|T_1\rangle$ state, where electron density is reduced at $s = 0$, thereby decreasing the energy.

2. Electron Hole Picture

The correlation function $g^{(2)}(s)$ involves all the electrons in the molecule, including many that in the tight-binding limit remain in the same single-particle states they inhabit in the ground state. So to identify the behavior of charges in the excited states we move to an electron-hole picture, which naturally focuses on the excitations. Of course, even the ground state $|g\rangle$, calculated with the inclusion of the Hubbard Hamiltonian, includes the virtual excitation of electron-hole pairs. However, we find that their populations in the ground state are very small, and hence we can expect that the correlations

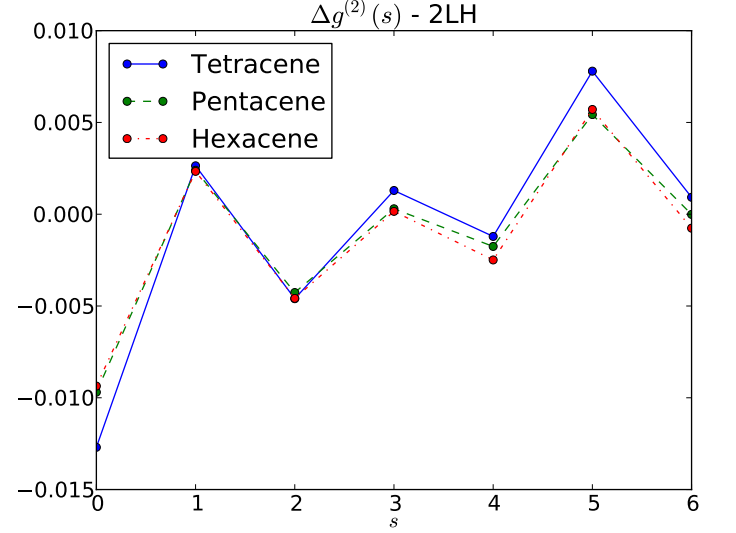


FIG. 7: $\Delta g^{(2)}(s)$ plotted for the first doubly excited $2LH$. The Hubbard interaction in this case stabilizes the $2LH$ state by decreasing electron density at $s = 0$ and pushing it further away in a manner reminiscent of the first triplet state (Fig 6).

of the electron and hole densities in the excited states do reliably characterize the nature of those states. The electron and hole densities are

$$n_{e\sigma}(i) = \sum_{mm'} \Gamma_{mm'}(i) a_{m\sigma}^\dagger a_{m'\sigma}, \quad (39)$$

and

$$n_{h\sigma}(i) = \sum_{mm'} \Gamma_{mm'}(i) b_{m\sigma}^\dagger b_{m'\sigma}, \quad (40)$$

and so the functions that track correlations between electrons and holes of different spins are

$$g_{e\uparrow h\downarrow}^{(2)}(i, j) = \frac{\langle n_{e\uparrow}(i) n_{h\downarrow}(j) \rangle}{\langle n_{e\uparrow}(i) \rangle \langle n_{h\downarrow}(j) \rangle}, \quad (41)$$

while those that track correlations between electrons and holes of the same spin are

$$g_{e\uparrow h\uparrow}^{(2)}(i, j) = \frac{\langle n_{e\uparrow}(i) n_{h\uparrow}(j) \rangle}{\langle n_{e\uparrow}(i) \rangle \langle n_{h\uparrow}(j) \rangle}. \quad (42)$$

We form the average quantities $g_{e\uparrow h\downarrow}^{(2)}(s)$ and $g_{e\uparrow h\uparrow}^{(2)}(s)$ as a function of the number of bond lengths s , as outlined in the previous section, and evaluate these quantities in both the tight-binding limit and with the inclusion of the Hubbard Hamiltonian. We focus on the doubly excited $2LH$ state, and show the results in Fig. 8.

There has been some speculation [1, 10] that the doubly excited state is somehow related to the singlet fission process. It is conjectured that upon excitation to the S_1 state, the excitation relaxes down to the $2LH$ state, which breaks up into two

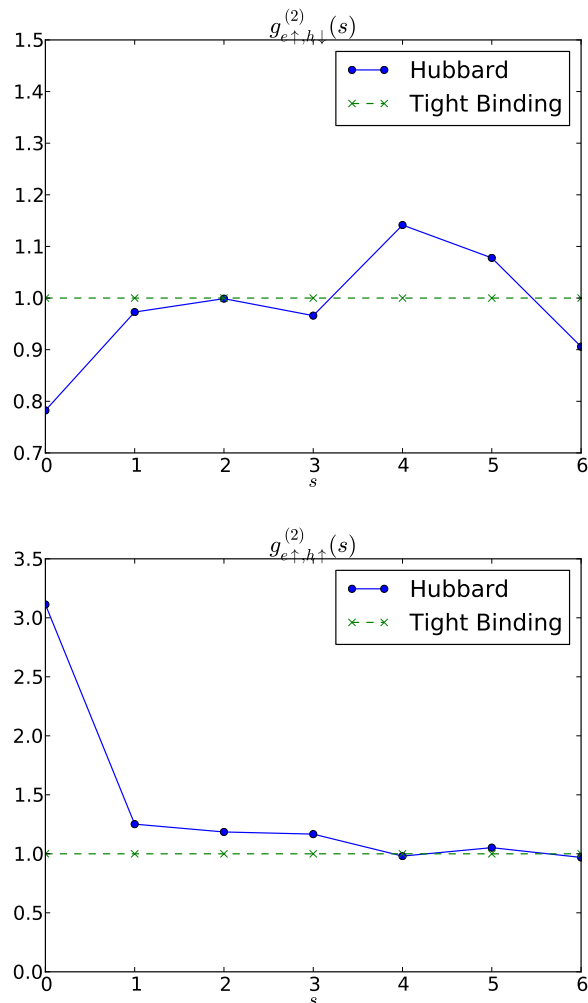


FIG. 8: The $g^{(2)}_{e\uparrow h\downarrow}(s)$ (top) and $g^{(2)}_{e\uparrow h\uparrow}(s)$ (bottom) is plotted as a function of electron-hole separation s for the first doubly excited state $2LH$, in pentacene. The steps are all scaled by the bond length l .

triplet excitons. In the tight-binding picture, one can always write $2LH$ as a product of two triplet excitons. However, as was discussed earlier, the tight-binding picture cannot distinguish between singlet and triplet states energetically. Unsurprisingly, the electron-hole density correlation function for the tight-binding $2LH$ state is uniform, that is, up electrons are equally as likely to be correlated with down holes as they are with up holes. The degeneracy of the triplet and singlet states is lifted by the introduction of Coulomb repulsion via the Hubbard Hamiltonian, which also alters the density correlation for the $2LH$ state; the electrons and holes of the same (different) spin avoid (seek) each other. This feature only becomes apparent when observing the electron-hole density correlation functions rather than the electron density correlation function.

While our calculations confirm that the $2LH$ state is indeed primarily composed of two electron-hole pairs and is close in energy to two times that of the triplet excitation, $2E(T_1)$ [1], it is not lower in energy than the S_1 state. It might be possible for this state to participate in the formation of two triplet excitons in the case of a pentacene dimer, however in the monomer case it cannot be involved in MEG. Our calculation qualitatively agrees with that of another, more sophisticated, calculation [4].

V. CONCLUSION

In this paper we have demonstrated a computationally and physically simple scheme to extract the electronic excited state energies as well as wavefunctions of π conjugated -acene molecules, specifically tetracene, pentacene and hexacene. A Hubbard model with a limited set of states was used to find these energies and wavefunctions. We have shown that the energies and oscillator strengths predicted by this model are in line with what one can achieve with modern quantum chemical techniques, but crucially without the computational complexity associated with these strategies. We also used our method to investigate the first doubly excited state, $2LH$, which is difficult to extract from quantum chemistry calculations. It has been speculated by some as being intimately involved in the singlet fission or multi-exciton generation process.

We introduced a density correlation function, $g^{(2)}(s)$, to analyze the nature of these states. The ground state exhibits features typical of a noninteracting 1D electron gas, with oscillations in the $g^{(2)}(s)$ with a wavelength of $\lambda = 2l$, where l is the bond length. The Hubbard interaction leads to the deepening of the correlation hole. The first doubly excited state, $2LH$, exhibits similar behavior. We found that the Hubbard interaction deepens the correlation hole in triplets (which are lower in energy) and increases the correlation hole in singlets (which are higher in energy).

A more physically intuitive electron-hole picture was then introduced and we computed the density correlation of electrons with holes; these density correlation functions were then used to characterize the first doubly excited state, $2LH$. In the $2LH$ state, the electrons and holes of the same spin seek each other while the electrons and holes of different spins avoid each other. This type of behavior is reminiscent of triplet like excitons. While the $2LH$ state is seemingly composed of two triplet like excitons, it is higher in energy than the S_1 state and as such, at least in the case of a monomer, it cannot participate in multi-exciton generation.

Acknowledgments

ZS thanks R. Schaffer, V. Venkataraman for edifying discussions.

Appendix A: The Total Hamiltonian in the Electron-Hole Basis

In the electron-hole basis the tight-binding Hamiltonian is

$$H_{TB} = \sum_{\substack{m \in \text{empty}, \\ \sigma}} \hbar\omega_m a_{m\sigma}^\dagger a_{m\sigma} - \sum_{\substack{m' \in \text{filled}, \\ \sigma}} \hbar\omega_{m'} b_{m'\sigma}^\dagger b_{m'\sigma} + 2 \sum_{k \in \text{filled}} \hbar\omega_k, \quad (\text{A1})$$

while the Hubbard Hamiltonian can be written as

$$H_{Hu} = \sum_{mm'pp'} \Gamma_{mm'pp'} C_{m\uparrow}^\dagger C_{m'\uparrow} C_{p\downarrow}^\dagger C_{p'\downarrow}, \quad (\text{A2})$$

where $\Gamma_{mm'pp'} = U \sum_i M_{im}^* M_{im'} M_{ip'}^* M_{ip}$. Moving to the electron-hole basis and normal ordering, the Hamiltonian can be expressed as

$$H = H_0 + H_1 + H_2 + H_3 + H_4. \quad (\text{A3})$$

The first component can be expressed as

$$H_0 = 2 \sum_{m \in \text{filled}} \hbar\omega_m + \sum_{\substack{l \in \text{filled}, \\ m \in \text{filled}}} \Gamma_{mml}. \quad (\text{A4})$$

The first part of Eq. A4 represents the tight-binding contribution of the nominal vacuum state $|0\rangle$ while the second part is the Coulomb repulsion of the tight-binding ground state.

The second part of the Hamiltonian is

$$\begin{aligned} H_1 = & \sum_{m\sigma} \hbar\omega_m a_{m\sigma}^\dagger a_{m\sigma} - \sum_{m'\sigma} \hbar\omega_{m'} b_{m'\sigma}^\dagger b_{m'\sigma} + \sum_{\substack{m \in \text{filled}, \\ pp'}} \Gamma_{mmp'p'} (a_{p\uparrow}^\dagger a_{p'\uparrow} + a_{p\downarrow}^\dagger a_{p'\downarrow}) \\ & - \sum_{\substack{m \in \text{filled}, \\ pp'}} \Gamma_{mmp'p'} (b_{p'\uparrow}^\dagger b_{p\uparrow} + b_{p'\downarrow}^\dagger b_{p\downarrow}). \end{aligned} \quad (\text{A5})$$

We have used the identity

$$\sum_{p \in \text{filled}} \Gamma_{mmp'p} = 0, \quad (\text{A6})$$

where p ranges over the filled states, to simplify H_1 . This identity is proved by

$$\sum_{p \in \text{filled}} \Gamma_{mmp'p} = \sum_i \sum_{p \in \text{filled}} M_{ip}^* M_{ip} M_{im}^* M_{im'}, \quad (\text{A7})$$

$$= \frac{1}{2} \sum_i M_{im}^* M_{im'} = 0. \quad (\text{A8})$$

Eq. A5 represents the single particle terms that play a role in the matrix elements of both single and double excitations. The third part of Hamiltonian is

$$\begin{aligned} H_2 = & \sum_{mm'pp'} \Gamma_{mm'pp'} \left(a_{p\downarrow}^\dagger b_{m\downarrow} - a_{p\uparrow}^\dagger b_{m\uparrow} \right) a_{m'\uparrow} a_{p'\downarrow} + \sum_{mm'pp'} \Gamma_{mm'pp'} a_{m\uparrow}^\dagger a_{p\downarrow}^\dagger \left(b_{p'\uparrow}^\dagger a_{m'\uparrow} - b_{p'\downarrow}^\dagger a_{m'\downarrow} \right), \\ & \sum_{mm'pp'} \Gamma_{mm'pp'} \left(b_{p'\downarrow}^\dagger a_{m'\downarrow} - b_{p'\uparrow}^\dagger a_{m'\uparrow} \right) b_{p\uparrow} b_{m\downarrow} + \sum_{mm'pp'} \Gamma_{mm'pp'} b_{m'\downarrow}^\dagger b_{p'\uparrow}^\dagger \left(a_{m\downarrow}^\dagger b_{p\downarrow} - a_{m\uparrow}^\dagger b_{p\uparrow} \right). \end{aligned} \quad (\text{A9})$$

While H_2 has matrix elements between tight-binding states that are in general non-zero, for the states and the active spaces investigated in this paper H_2 does not contribute. The fourth part of the Hamiltonian is

$$\begin{aligned} H_3 = & - \sum_{mm'pp'} \Gamma_{mm'pp'} \left(a_{p\downarrow}^\dagger b_{m'\downarrow}^\dagger b_{m\downarrow} a_{p'\downarrow} + a_{p\uparrow}^\dagger b_{m'\uparrow}^\dagger b_{m\uparrow} a_{p'\uparrow} \right), \\ & + \sum_{mm'pp'} \Gamma_{mm'pp'} \left(a_{m\downarrow}^\dagger b_{m'\uparrow}^\dagger b_{p\downarrow} a_{p'\uparrow} + a_{m\uparrow}^\dagger b_{m'\downarrow}^\dagger b_{p\uparrow} a_{p'\downarrow} \right), \\ & - \sum_{mm'pp'} \Gamma_{mm'pp'} \left(b_{m\downarrow} b_{p\uparrow} a_{m'\uparrow} a_{p'\downarrow} + a_{m\uparrow}^\dagger a_{p\downarrow}^\dagger b_{m'\downarrow}^\dagger b_{p'\uparrow}^\dagger \right). \end{aligned} \quad (\text{A10})$$

The term H_3 (Eq. (A10)) represents the part of the Hamiltonian that has a contribution to the matrix elements between single excitations, between the ground state and double excitations, as well as between different double excitations.

The last part of the Hamiltonian is written as

$$H_4 = \sum_{mm'pp'} \Gamma_{mm'pp'} a_{p\downarrow}^\dagger a_{m\uparrow}^\dagger a_{m'\uparrow} a_{p'\downarrow} + \sum_{mm'pp'} \Gamma_{mm'pp'} b_{m'\downarrow}^\dagger b_{p'\uparrow}^\dagger b_{p\uparrow} b_{m\downarrow}. \quad (\text{A11})$$

H_4 (Eq. (A11)) is the part of the Hamiltonian which contributes to the matrix elements between double excitations only.

Appendix B: Dipole Operator in the electron-hole Basis

Neglecting overlap between neighboring p_z orbitals, the dipole moment operator of a molecule with nuclei assumed fixed is given by

$$\boldsymbol{\mu} = \sum_i e \mathbf{r}_i \left(\sum_\sigma c_{i\sigma}^\dagger c_{i\sigma} - 1 \right), \quad (\text{B1})$$

where \mathbf{r}_i is the position of site i from any chosen origin, $e = -|e|$ is the electronic charge, and the charge of each nucleus not balanced by the in-plane bonding electrons of the molecule is included so the dipole moment operator is independent of origin. Transforming to the tight-binding basis, the α^{th} Cartesian component of the dipole moment is

$$\mu^\alpha = \left(\sum_{mm'} \mu_{mm'}^\alpha (C_{m\uparrow}^\dagger C_{m'\uparrow} + C_{m\downarrow}^\dagger C_{m'\downarrow}) \right) - \sum_i e r_i^\alpha, \quad (\text{B2})$$

where the operators $C_{m\sigma}^\dagger$ and $C_{m\sigma}$ are defined by Eqs. (4, 5) respectively. The quantity $\mu_{mm'}^\alpha$ is the α^{th} component of the electronic contribution to the dipole matrix element between two tight binding states m and m' which is

$$\mu_{mm'}^\alpha = e \sum_i r_i^\alpha M_{im}^* M_{im'}, \quad (\text{B3})$$

where the sum ranges over all sites i , r_i^α is the position of the α^{th} coordinate of site i , and M_{im} is the amplitude of the i^{th} site for the m^{th} tight-binding state. In the electron-hole picture, the α^{th} component of the dipole operator (B2) is

$$\mu^\alpha + \sum_i e r_i^\alpha = \mu_1^\alpha + \mu_2^\alpha + \mu_3^\alpha, \quad (\text{B4})$$

where

$$\mu_1^\alpha = \sum_{mm'} \mu_{mm'}^\alpha (a_{m\uparrow}^\dagger a_{m'\uparrow} + a_{m\downarrow}^\dagger a_{m'\downarrow}), \quad (\text{B5})$$

$$\mu_2^\alpha = - \sum_{mm'} \mu_{mm'}^\alpha (b_{m'\uparrow}^\dagger b_{m\uparrow} + b_{m'\downarrow}^\dagger b_{m\downarrow}), \quad (\text{B6})$$

$$\mu_3^\alpha = \sum_{mm'} \mu_{mm'}^\alpha (a_{m\uparrow}^\dagger b_{m'\downarrow}^\dagger + a_{m\downarrow}^\dagger b_{m'\uparrow}^\dagger + b_{m'\downarrow} a_{m\uparrow} + b_{m'\uparrow} a_{m\downarrow}). \quad (\text{B7})$$

Appendix C: Decreasing the number of basis states and its impact on transition energies and density correlation functions

We have investigated the effect of decreasing the size of the basis on the transition energies and density correlation functions of pentacene. The basis we use in the text we denote as the “full active space” or FAS. This is composed of all single excitations of the form of Eq. (10) and all double excitations of the form of Eq. (19). The levels involved are H_3 to L_3 .

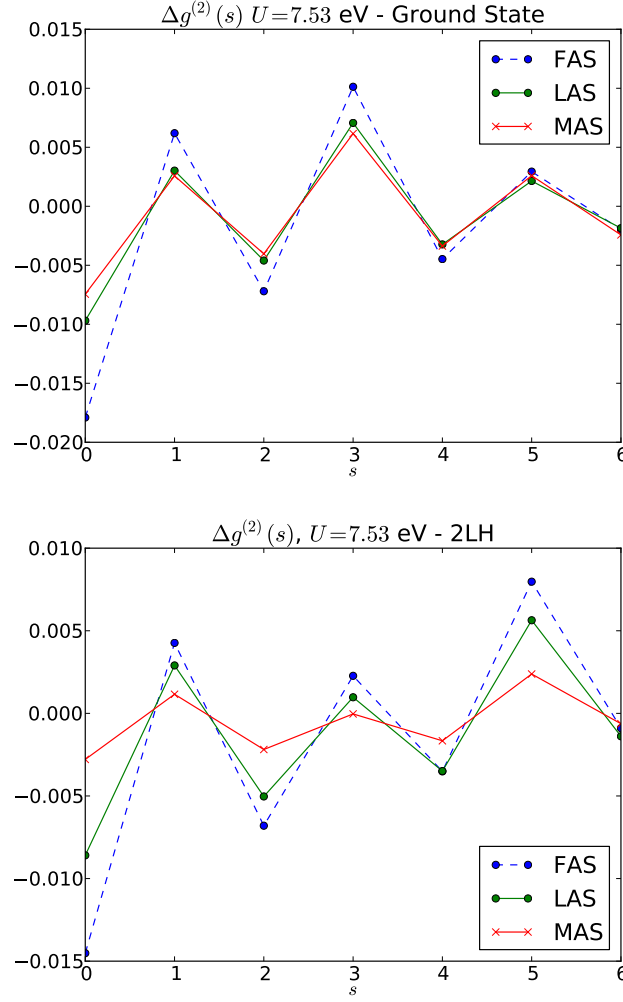


FIG. 9: $\Delta g^{(2)}(s)$ of pentacene plotted for both the ground (top) and $2LH$ state (bottom) for three different active spaces, MAS, LAS and FAS. Qualitatively, decreasing the size of the basis has little impact on the density correlation of the ground and the $2LH$ state. In these plots, we fix the value of the Hubbard parameter at $U = 7.53$ eV, the value for which the first singlet transition matches the literature value for the MAS basis.

We have considered two smaller basis sets. The first of these consists of all single excitations of the form of Eq. (10) and all the double excitations of the form Eq. (19), but involving only the levels H_1 to L_1 . We call this basis set the “limited active space”, or LAS. The other basis set we used consists of select single and double excitations from the LAS. This basis is called the “minimum active space”, or MAS. The double excitations included in the MAS are

$$|2LH\rangle = a_{L\uparrow}^\dagger a_{L\downarrow}^\dagger b_{H\downarrow}^\dagger b_{H\uparrow}^\dagger |0\rangle, \quad (C1)$$

$$|2LH_1\rangle = a_{L\uparrow}^\dagger a_{L\downarrow}^\dagger b_{H_1\downarrow}^\dagger b_{H_1\uparrow}^\dagger |0\rangle, \quad (C2)$$

$$|2L_1H\rangle = a_{L_1\uparrow}^\dagger a_{L_1\downarrow}^\dagger b_{H\downarrow}^\dagger b_{H\uparrow}^\dagger |0\rangle, \quad (C3)$$

$$|2L_1H_1\rangle = a_{L_1\uparrow}^\dagger a_{L_1\downarrow}^\dagger b_{H_1\downarrow}^\dagger b_{H_1\uparrow}^\dagger |0\rangle, \quad (C4)$$

$$|\overline{LL_1}; HH_1\rangle = a_{L\uparrow}^\dagger a_{L_1\downarrow}^\dagger b_{H\downarrow}^\dagger b_{H_1\uparrow}^\dagger |0\rangle, \quad (C5)$$

$$|\overline{L_1L}; H_1H\rangle = a_{L_1\uparrow}^\dagger a_{L\downarrow}^\dagger b_{H_1\downarrow}^\dagger b_{H\uparrow}^\dagger |0\rangle, \quad (C6)$$

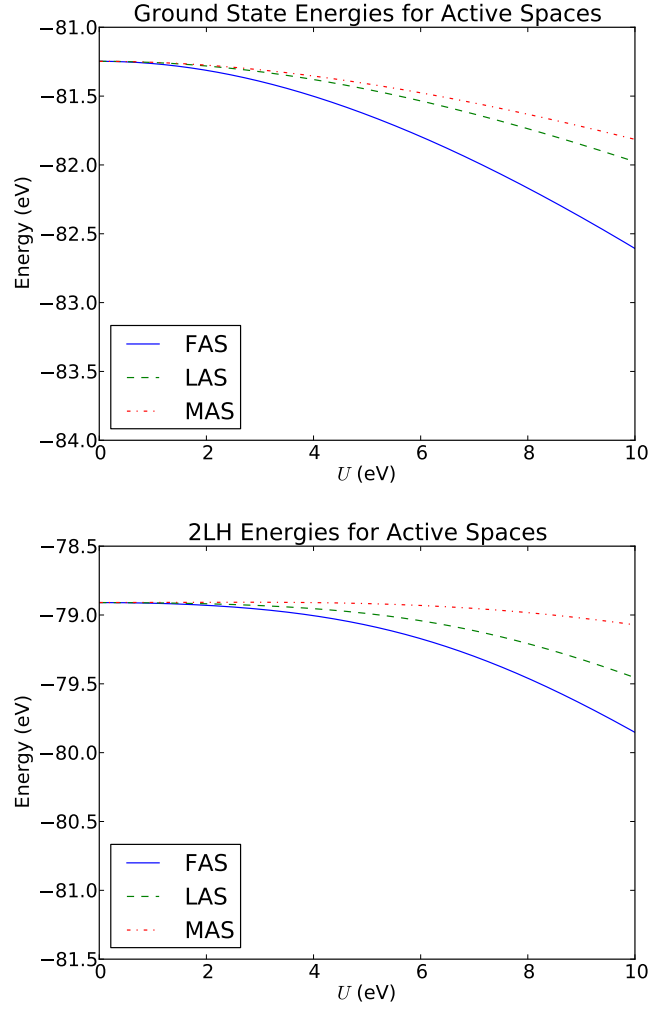


FIG. 10: Absolute energies of the ground (top) and 2LH state (bottom) plotted as a function of U for various active spaces.

and single excitations included are

$$|\overline{LH}, \sigma\rangle = a_{L\sigma}^\dagger b_{H\bar{\sigma}}^\dagger |0\rangle, \quad (C7)$$

$$|\overline{L_1H_1}, \sigma\rangle = a_{L_1\sigma}^\dagger b_{H_1\bar{\sigma}}^\dagger |0\rangle, \quad (C8)$$

$$|\overline{LH_1}, \sigma\rangle = a_{L\sigma}^\dagger b_{H_1\bar{\sigma}}^\dagger |0\rangle, \quad (C9)$$

$$|\overline{L_1H}, \sigma\rangle = a_{L_1\sigma}^\dagger b_{H\bar{\sigma}}^\dagger |0\rangle, \quad (C10)$$

$$|\overline{L_2H}, \sigma\rangle = a_{L_2\sigma}^\dagger b_{H\bar{\sigma}}^\dagger |0\rangle, \quad (C11)$$

$$|\overline{L_3H}, \sigma\rangle = a_{L_3\sigma}^\dagger b_{H\bar{\sigma}}^\dagger |0\rangle, \quad (C12)$$

$$|\overline{LH_2}, \sigma\rangle = a_{L\sigma}^\dagger b_{H_2\bar{\sigma}}^\dagger |0\rangle, \quad (C13)$$

$$|\overline{LH_3}, \sigma\rangle = a_{L\sigma}^\dagger b_{H_3\bar{\sigma}}^\dagger |0\rangle. \quad (C14)$$

The density correlation functions for the ground and 2LH state are plotted in Fig. 9 for a value of U such that the S_1 transition energy matches the literature value in pentacene for the MAS basis. As we reduce the size of the basis, there is little qualitative difference in the density correlation function of these states. The transition energies for the various basis sets are shown in Table IV. The absolute energies of the ground and 2LH state are plotted in Fig. 10.

Basis	U (eV)	T_1 (eV)	$2LH$ (eV)	$g \rightarrow S_1$ oscillator strength	$S_1 \rightarrow 2LH$ oscillator strength
MAS	7.53	0.74	2.63	0.127	0.102
LAS	7.00	0.84	2.52	0.131	0.0691
PAS	5.80	1.06	2.61	0.146	0.0877

TABLE IV: Transition energies of the first triplet and the first doubly excited state of pentacene for various basis sets. We choose a U such that the first singlet transition matches experiment. Hence for each basis the value of U is different.

-
- [1] P.M. Zimmerman, Z. Zhang, C.B. Musgrave, *Nature Chemistry* **2**, 648, (2010)
- [2] M. Shapiro and P. Brumer, *Principles of the Quantum Control of Molecular Processes* John Wiley, New York (2003)
- [3] I. Paci, J.C. Johnson, X.D. Chen, G. Rana, D. Popovic, D.E. David, A.J. Nozik, M.A. Ratner, J. Michl, *J. Am. Chem. Soc.*, **128**, 16546-16553 (2006)
- [4] T. Zeng, R. Hoffmann, N. Ananth, *J. Am. Chem. Soc.*, **136**, 5755-5764 (2014)
- [5] C. Raghu, Y. Anusooya Pati, S. Ramasesha, *Phys. Rev. B* **65**, 155204 (2002)
- [6] Burak Himmetoglu, Andrea Floris, Stefano de Gironcoli, Matteo Cococcioni, arXiv:1309.3355
- [7] W. Barford, *Electronic and Optical Properties of Conjugated Polymers* Oxford University Press, New York (2005)
- [8] T. C. Berkelbach, M. S. Hybertsen, D. R. Reichman, arXiv: 1211.6459v1
- [9] T. C. Berkelbach, M. S. Hybertsen, D. R. Reichman, arXiv: 1211.6458
- [10] W.-L. Chan, M. Ligges, A. Jailaubekov, L. Kaake, L. Miaja-Avila, X.-Y. Zhu, *Science* **334**, 1541, (2011)
- [11] W.-L. Chan, M. Ligges, X.-Y. Zhu, *Nature Chemistry* **4**, 840 (2012)
- [12] M. Schuler, M. Rosner, T. O. Wehling, A. I. Lichtenstein, M. I. Katsnelson, *Phys. Rev. Lett.* **111**, 036601 (2013)
- [13] R. A. Muniz, J.E. Sipe, *Phys. Rev. B* **89**, 205113 (2014)
- [14] K.M. Rao, J.E. Sipe, *Phys. Rev. B* **86**, 115427 (2012)
- [15] J. Rioux, J.E. Sipe, *Physica E* **45** 1-15 (2012)
- [16] J. Rioux, G. Burkard, J.E. Sipe, *Phys. Rev. B* **83**, 195406 (2011)
- [17] V. M. Agranovich, *Excitations in Organic Solids*, (Oxford University Press, Oxford 2009).
- [18] T.E. Brown, *et al.*, *Chemistry, The Central Science*, (Prentice Hall, New York 2011).
- [19] H. Yamagata, J. Norton, E. Hontz, Y. Olivier, D. Beljonne, J. L. Brédas, R. J. Silbey, F. C. Spano, *J. Chem. Phys.*, **134**, 204703 (2011)
- [20] A. Völcker, H.-J. Adick, R. Schmidt, H.-D. Braue, *Chem. Phys. Lett.*, **159**, 103-108 (1989)
- [21] J. Burgos, M. Pope, C.E. Swenberg, R.R. Alfano, *Phys. Status Solidi B.*, **83**, 249-256 (1977)
- [22] Yu.F. Pedash, O.V. Prezhdo, S.I. Kotelevskiy, V.V. Prezhdo, *J. Mol. Struc. (Theochem)*, **585**, 49-59 (2002)
- [23] R. Kundu, arXiv: 0907.4264v1
- [24] R.G Endres, C.Y Fong, L.H Yang, G Witte, Ch Wöll, *Comp. Mat. Sci.*, **29**, 362-370 (2004)
- [25] D. Pines, *Elementary Excitations in Solids*, (W.A. Benjamin Inc., New York 1977)
- [26] G. F. Giuliani, G. Vignale, *Quantum Theory of the Electron Liquid*, (Cambridge University Press, New York, 2005)
- [27] H. Angliker, E. Rommel, J. Wirz, *Chem. Phys. Lett.*, **87**, 208, (1982)
- [28] M. B. Smith, J. Michl, *Ann. Rev. Phys. Chem.*, **64**, 361-386, (2013)
- [29] by a direct mechanism we mean the lowest singlet state S_1 relaxes down to two T_1 states, with T_1 being the lowest triplet state.
- [30] by this we mean the initial S_1 excitation relaxes or is coupled to an intermediate doubly excited state which then relaxes down to two triplet T_1 states.